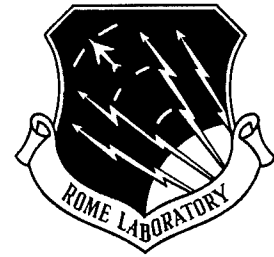


**RL-TR-96-244**  
**In-House Report**  
**May 1997**



# **ULTRAFAST COMPONENTS FOR OPTICAL INTERCONNECTS**

**Michael J. Hayduk, Steven T. Johns, Mark F. Krol**  
**(Rome Laboratory) and Walter Kaechele (Rensselaer**  
**Polytechnic Institute)**

*APPROVED FOR PUBLIC RELEASE; DISTRIBUTION UNLIMITED.*

**19970715 213**

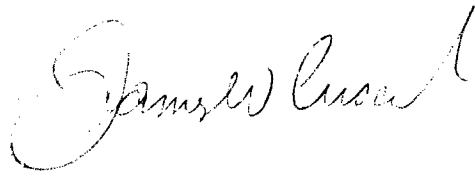
**DTIC QUALITY INSPECTED 4**

**Rome Laboratory**  
**Air Force Materiel Command**  
**Rome, New York**

This report has been reviewed by the Rome Laboratory Public Affairs Office (PA) and is releasable to the National Technical Information Service (NTIS). At NTIS it will be releasable to the general public, including foreign nations.

RL-TR-96-244 has been reviewed and is approved for publication.

APPROVED:



JAMES W. CUSACK  
Chief, Photonics Division  
Surveillance & Photonics Directorate

FOR THE COMMANDER:



FRED J. DEMMA, Acting Director  
Surveillance & Photonics Directorate

If your address has changed or if you wish to be removed from the Rome Laboratory mailing list, or if the addressee is no longer employed by your organization, please notify Rome Laboratory/OCPA, Rome, NY 13441. This will assist us in maintaining a current mailing list.

Do not return copies of this report unless contractual obligations or notices on a specific document require that it be returned.

<b>REPORT DOCUMENTATION PAGE</b>			Form Approved OMB No. 0704-0188	
Public reporting burden for this collection of information is estimated to average 1 hour per response, including the time for reviewing instructions, searching existing data sources, gathering and maintaining the data needed, and completing and reviewing the collection of information. Send comments regarding this burden estimate or any other aspect of this collection of information, including suggestions for reducing this burden, to Washington Headquarters Services, Directorate for Information Operations and Reports, 1215 Jefferson Davis Highway, Suite 1204, Arlington, VA 22202-4302, and to the Office of Management and Budget, Paperwork Reduction Project (0704-0188), Washington, DC 20503.				
1. AGENCY USE ONLY (Leave blank)	2. REPORT DATE May 1997	3. REPORT TYPE AND DATES COVERED <b>FINAL, Oct 95 - Sep 96 (In-House)</b>		
4. TITLE AND SUBTITLE  <b>ULTRAFast COMPONENTS FOR OPTICAL INTERCONNECTS</b>		5. FUNDING NUMBERS  C - NA PE - 62702F PR - 4600 TA - P1 WU - 17		
6. AUTHOR(S)  <b>Michael J. Hayduk, Steven T. Johns, Mark F. Krol (Rome Laboratory) Walter Kaechele (Rensselaer Polytechnic Institute)</b>				
7. PERFORMING ORGANIZATION NAME(S) AND ADDRESS(ES)  <b>Rome Laboratory/OCPA 25 Electronic Pky Rome NY 13441-4515</b>		8. PERFORMING ORGANIZATION REPORT NUMBER		
9. SPONSORING / MONITORING AGENCY NAME(S) AND ADDRESS(ES) <b>Rome Laboratory/OCPA 25 Electronic Pky Rome NY 13441-4515</b>		10. SPONSORING / MONITORING AGENCY REPORT NUMBER  RL-TR-96-244		
11. SUPPLEMENTARY NOTES  <b>Rome Laboratory Project Engineer: Michael J. Hayduk, OCPA, 315-330-7753</b>				
12a. DISTRIBUTION AVAILABILITY STATEMENT  <b>APPROVED FOR PUBLIC RELEASE; DISTRIBUTION UNLIMITED</b>		12b. DISTRIBUTION CODE		
13. ABSTRACT (Maximum 200 words) <b>This report describes the results of experiments performed in various areas of material and component technology required for the development of multiple gigabit per second fiber-based optical interconnect and optical communication links. First, we will summarize the development of a chromium-doped:YAG (Cr<sup>4+</sup>:YAG) solid-state laser for use in the 1500 nm transmission window of optical fiber. The Cr<sup>4+</sup>:YAG laser produces tunable femtosecond pulses from 1488 to 1535 nm with average TEM<sub>00</sub> output powers ranging from 40 to 80 mW. The laser is mode-locked using a novel saturable absorber mirror structure. The laser is also tunable from 1450 to 1574 nm in the continuous-wave mode with an average TEM<sub>00</sub> output power of 600 mW at 1487 nm. Next, we will describe the synchronization of a passively mode-locked erbium-doped fiber laser to an actively mode-locked fiber ring laser. Stable synchronization is obtained at injection powers of 1.5 mW. Finally, we report on the investigation of multiple quantum well saturable absorbers used to initiate mode-locking of standing-wave linear cavity erbium-doped fiber lasers.</b>				
14. SUBJECT TERMS <b>solid-state laser, mode-locked, semiconductor, saturable absorber, multiple quantum wells, fiber laser, synchronization</b>		15. NUMBER OF PAGES 36		
		16. PRICE CODE		
17. SECURITY CLASSIFICATION OF REPORT <b>UNCLASSIFIED</b>	18. SECURITY CLASSIFICATION OF THIS PAGE <b>UNCLASSIFIED</b>	19. SECURITY CLASSIFICATION OF ABSTRACT <b>UNCLASSIFIED</b>	20. LIMITATION OF ABSTRACT  <b>UNLIMITED</b>	

## Table of Contents

<u>Section</u>	<u>Page</u>
Preface	ii
1. Introduction	1
2. Chromium-doped:YAG Laser Development in the 1500 nanometer Region	2
3. Investigation of Synchronized Mode-Locked Fiber Lasers	13
4. Linear Optical Properties of Quantum Well Structures Near 1550 nanometers	17
5. References	24
6. Acknowledgments	25

## **Preface**

The authors contributed equally to the work discussed in this report. The femtosecond chromium-doped:YAG laser was developed by M. Hayduk, M. Krol and S. Johns. W. Kaechele and M. Krol investigated the performance of synchronized fiber lasers. The linear optical properties of quantum well saturable absorbers were analyzed by M. Hayduk, M. Krol and S. Johns.

## 1. Introduction

Optical interconnects are a means of alleviating the electronic input/output (I/O) bottleneck inherent in ultrafast communication systems. Previous studies have indicated that there are numerous deficiencies associated with commercially available components used in optical interconnect testbeds.[1] Development of ultrafast novel materials and devices (electro-optic modulators, demultiplexors, and pulsed sources) is therefore required for the continued improvement of multi-gigabit optical interconnect and communication systems. In particular, optoelectronic components are required which are directly compatible with integrated electronic circuits to develop compact, low-power interconnect and communication systems. Additionally, compact and rugged pulsed laser sources are required for optical interconnect systems. These laser sources must be compact and easily integrated with fiber-based systems.

The work performed in the current work unit can be summarized by three major efforts as follows.

1. The development of a tunable femtosecond chromium-doped YAG laser in the 1500 nanometer region for use in the characterization and testing of materials and devices for fiber-based interconnects.[2]
2. The use of harmonically mode-locked erbium-doped fiber lasers to injection seed a linear erbium-doped fiber laser cavity producing a synchronized pulse train. Synchronization of multiple lasers is crucial to the development of improved fiber-based interconnect schemes including time-division and wavelength-division multiplexing.[3]
3. The investigation of the linear optical properties of semiconductor quantum well structures near 1550 nanometers. These quantum well structures are used as saturable absorbers to mode-lock a standing wave erbium-doped fiber laser producing pulses on the order of 6 picoseconds. A more thorough understanding of the linear optical properties of the saturable absorbers will result in optimization

of the quantum well structures leading to improved mode-locking of the fiber laser.[4]

Each of these efforts has resulted in a significant contribution to the development and design of multiple gigahertz bandwidth fiber-based optical interconnects. However, the use of the chromium-doped:YAG laser and mode-locked erbium-doped fibers lasers is not solely limited to fiber-based optical interconnects. Other potential applications of these continuous-wave and pulsed sources include fiber sensing, ranging and biomedical diagnostics.

## **2. Chromium-doped:YAG Laser Development in the 1500 nanometer Region**

Novel devices such as electro-optic modulators and demultiplexors often contain quantum well structures which have thickness' less than 100 angstroms. These devices are fabricated by advanced growth techniques such as molecular beam epitaxy. The thickness and composition of these structures must be tightly controlled. However, multiple growth runs in the device development process are often required to refine the thickness and multiple layer composition. The use of a tunable laser source operating either in the continuous-wave (cw) or pulsed mode greatly aids in the device characterization and development process. The tunability of the laser allows the device to analyzed at multiple wavelengths. Using this data the growth of the device could then be optimized so that it operates at its specific design wavelength. The use of a tunable laser eliminates the need for multiple growth runs of the devices.

The use of chromium-doped:yttrium aluminum garnet ( $\text{Cr}^{4+}$ :YAG) as a lasing medium at room temperature was first demonstrated by Shestakov *et al.*[5] In this solid-state crystal, the tetravalent chromium ion serves as the lasing center.  $\text{Cr}^{4+}$ :YAG is an attractive alternative to color center lasers which are also tunable throughout the 1500 nm region but must be operated at cryogenic temperatures. The absorption band of  $\text{Cr}^{4+}$ :YAG is between 900 and 1100 nm making a neodymium-doped:yttrium aluminum garnet (Nd:YAG) laser operating at 1064 nm a convenient pump laser source. Figure 1 shows the emission spectra of the  $\text{Cr}^{4+}$ :YAG crystal that was used in our laser cavity. This emission spectra was taken using a Quantronix 116 Nd:YAG laser operating

at 1064 nm as the excitation source and a 0.275 meter ARC monochromator in conjunction with a germanium detector to collect the spectral data. The large spectral emission bandwidth shows that the  $\text{Cr}^{4+}$ :YAG crystal can be used as a lasing medium with wide tunability extending throughout the 1500 nm region.

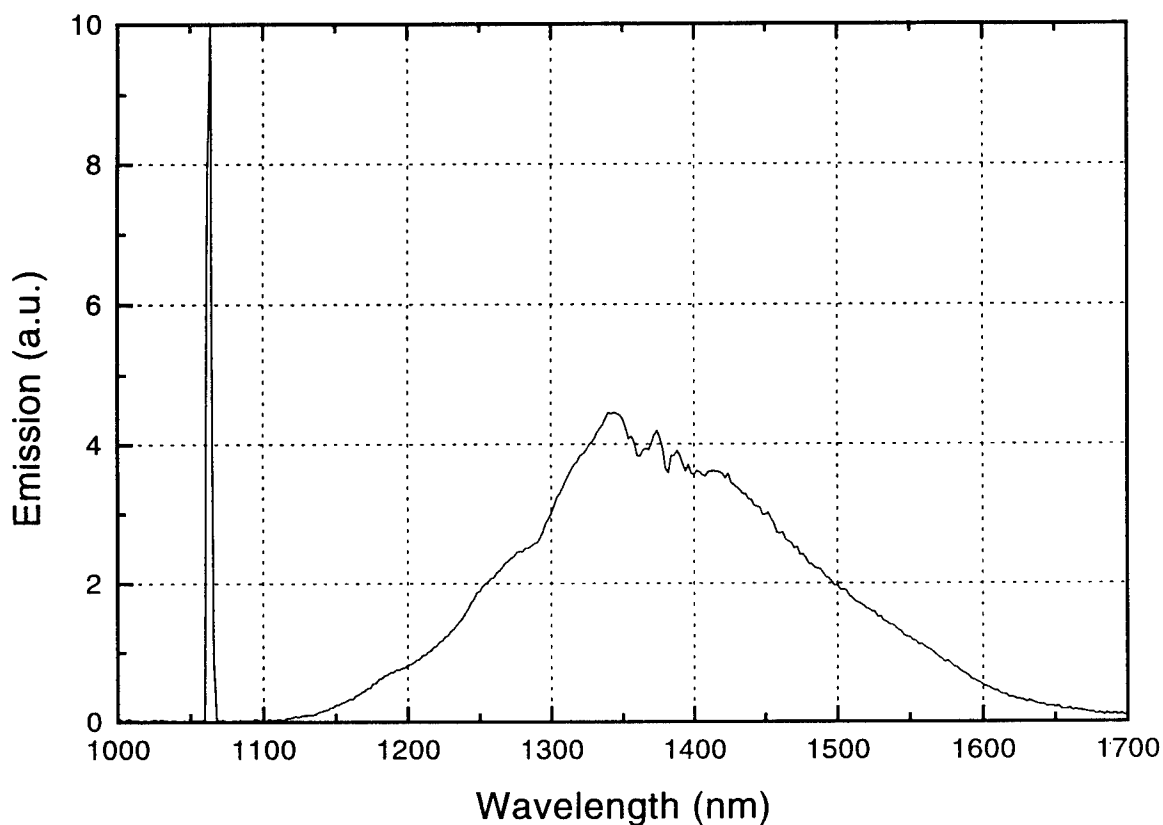


Figure 1. Emission spectrum of  $\text{Cr}^{4+}$ :YAG crystal pumped with 1064 nm Nd:YAG laser

The cw  $\text{Cr}^{4+}$ :YAG laser system consists of a nearly symmetric X-fold cavity as shown in Figure 2. The cavity layout is very similar to that of a standard titanium:sapphire laser. The Brewster-angled cylindrical  $\text{Cr}^{4+}$ :YAG laser crystal was obtained from the IRE-POLUS Institute. The  $\text{Cr}^{4+}$ :YAG rod which is 5 mm in diameter and 20 mm long was wrapped in indium foil and clamped in a brass housing to provide efficient heat removal. Using a thermal electric cooler under the brass housing, the temperature of the crystal was maintained at 15°C. The laser rod was placed



slightly off center between two highly reflecting focusing mirrors ( $R > 99.9\%$  from 1350 to 1550 nm) each of 10 cm radius of curvature. The angle of each focusing mirror was set to approximately  $15^\circ$  to compensate for the astigmatism introduced by the 20 mm  $\text{Cr}^{4+}:\text{YAG}$  rod. A plane wedged output coupler having 2% transmission was used. The overall cavity length is 1.58 m corresponding to an overall cavity repetition rate of 95 MHz. The laser was pumped by a Quantronix 416 Nd:YAG laser at 1064 nm that is focused into the gain medium by a 17.5 cm focal length, anti-reflection coated mode-matching lens. The lens was chosen so as to maximize the overlap between the pump and lasing volumes in the  $\text{Cr}^{4+}:\text{YAG}$  rod. Optimization of the mode-matching is critical in obtaining the most efficient cw operation of the laser.

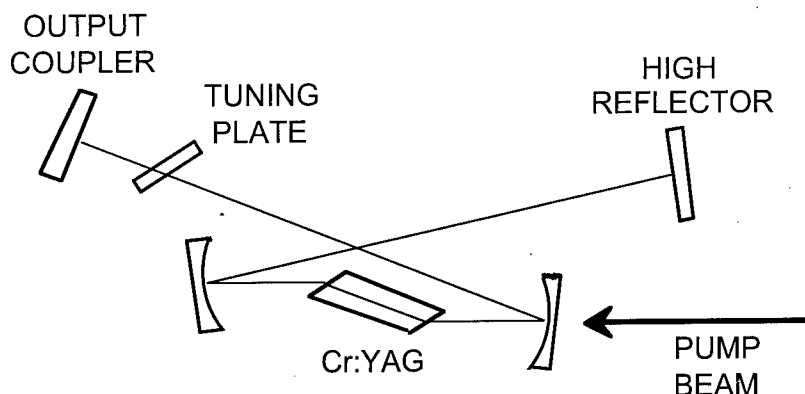


Figure 2. Schematic of continuous-wave  $\text{Cr}^{4+}:\text{YAG}$  laser X-cavity

The initial lasing of the  $\text{Cr}^{4+}:\text{YAG}$  system was achieved by 'chopping' the pump beam at a 50% duty cycle. The fluorescence signal was monitored at the back of the output coupler by a Newport 818-IR germanium p-i-n detector attached to an analog oscilloscope set to a long time scale. The focusing mirrors and position of the crystal were then adjusted to maximize the fluorescence. Upon optimization of the retro-reflected fluorescence beams from the output coupler and high reflector, lasing was achieved. Once the lasing signal was maximized, 'chopping' of the pump beam was no longer necessary and was removed.

In cw operation approximately 600 mW of TEM<sub>00</sub> power was obtained at 1487 nm. Tuning of the cavity could be achieved using two different intracavity elements. The first configuration is to place a fused silica prism before the high reflector. Using the prism we were able to tune the laser from 1446 to 1536 nm. The second configuration used a 0.6 mm thick quartz birefringent tuning plate placed before the output coupler. The tuning plate allowed us to continuously tune from 1450 to 1574 nm as shown in Figure 3. Further optimization of the laser cavity at the longer wavelengths allowed the tuning range to extend to approximately 1590 nm. The quartz tuning plate appears to be the tuning element of choice especially on the long wavelength side and easily covers the 1550 nm transmission window of optical fiber.

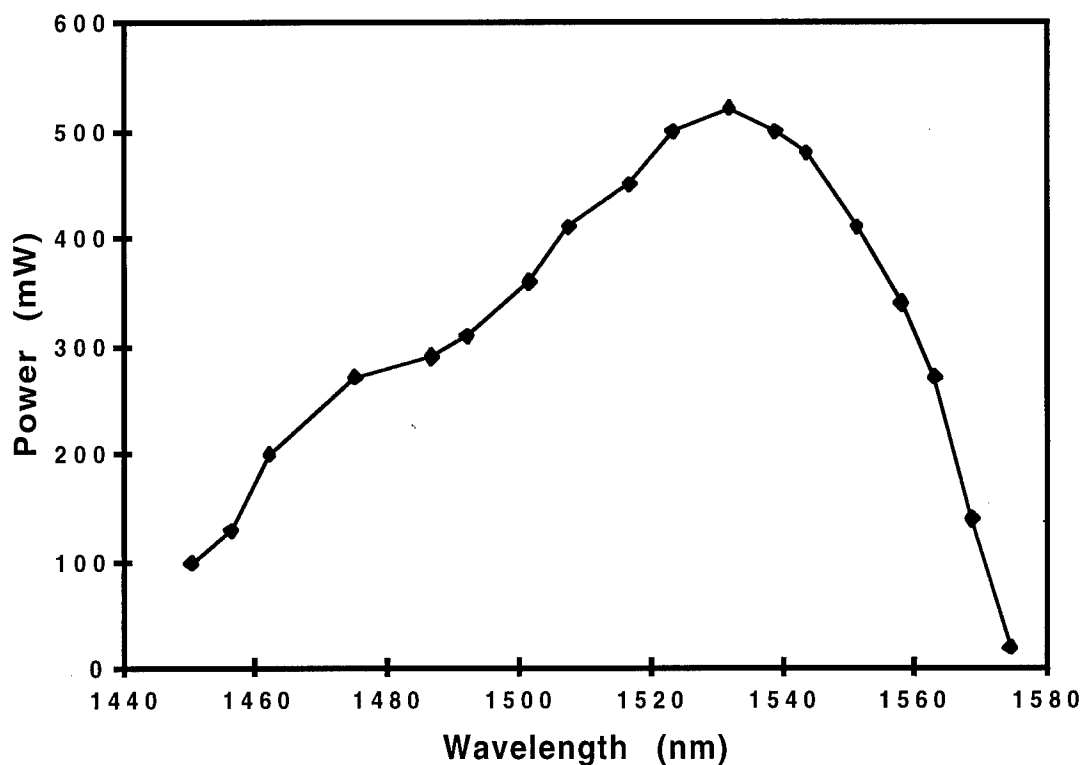


Figure 3. CW tuning range of Cr<sup>4+</sup>:YAG laser

Generation of ultrashort optical pulses with the  $\text{Cr}^{4+}$ :YAG laser has been achieved by many research groups in variety of ways. These methods include active mode-locking using an acousto-optic modulator (AOM)[6], self-starting Kerr lens mode-locking (KLM)[7], and regenerative mode-locking whereby a feedback control circuit drives an AOM[8]. Initiation of mode-locking using an intra-cavity AOM is not easily achieved because the low gain of the  $\text{Cr}^{4+}$ :YAG rod renders the system intolerant to excess loss mechanisms. The self-starting KLM technique does not require an AOM and has been shown to demonstrate pulses as short as 53 fs.[7] This method of mode-locking solid-state lasers utilizes the intensity dependent refractive index of the lasing medium to modify the transverse beam parameters of the cavity resulting in intensity dependent gain modulation. The gain modulation is provided by either a soft aperture generated by the pump-beam defined gain profile in the lasing medium or an actual intracavity hard aperture. As a result, the KLM process is highly sensitive to cavity alignment and is easily perturbed by mechanical vibrations and pump power fluctuations. A more reliable process of mode-locking solid-state lasers has been recently demonstrated which relies upon the use of a saturable absorber to start and stabilize the soliton formation process.[9,10] The saturable absorber eliminates the need for critical cavity alignment and renders mode-locked operation more tolerant to external perturbations.

The mode-locking of our  $\text{Cr}^{4+}$ :YAG laser at Rome Laboratory was achieved using a saturable absorber mirror (SAM) structure within the laser cavity. A schematic of this structure is shown in Figure 4. The SAM was grown by molecular beam epitaxy (MBE) on an undoped (100) GaAs substrate using a Varian Gen-II solid-source MBE system. The SAM consists of a distributed Bragg reflector with 24.5 periods of 132.1 nm AlAs low index/ 113.3 nm GaAs high index quarter-wave layers. A 20 nm  $\text{Al}_{0.48}\text{In}_{0.52}\text{As}$  buffer layer was grown on top of the partial Bragg stack. The saturable absorber region followed the buffer layer and is composed of the following double quantum well structure: 7 nm  $\text{Ga}_{0.47}\text{In}_{0.53}\text{As}$  well / 8 nm  $\text{Al}_{0.48}\text{In}_{0.52}\text{As}$  barrier / 7 nm  $\text{Ga}_{0.47}\text{In}_{0.53}\text{As}$  well. The entire structure is capped by a 74.1 nm  $\text{Al}_{0.48}\text{In}_{0.52}\text{As}$  layer. The total thickness of the buffer layer, the saturable absorber region and the cap layer were chosen so that a

high index quarter-wave layer is formed, thus completing the Bragg reflector. The width of the  $\text{Ga}_{0.47}\text{In}_{0.53}\text{As}$  wells were chosen to

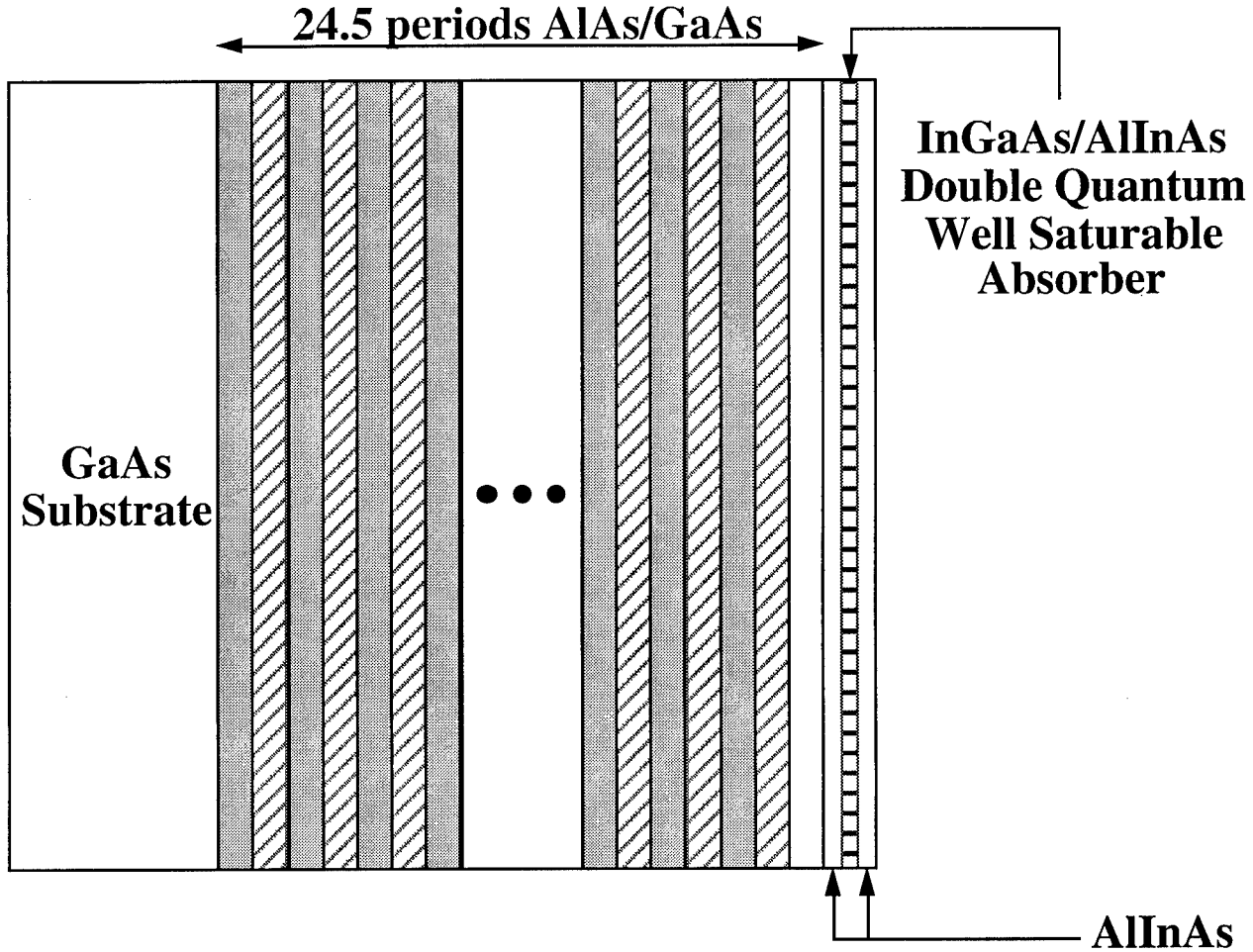


Figure 4. Schematic of saturable absorber mirror

place the bandedge, i.e. the heavy hole exciton absorption resonance, at a wavelength of 1500 nm. Two quantum wells were used to increase the nonlinear reflectance of the SAM. The quantum wells were placed near the peak of the electric field distribution in the first layer of the reflector resulting in a low quantum well saturation intensity. The measured reflectance spectrum of the SAM is shown in Figure 5. The peak reflectance is 99.9% centered at a wavelength of 1530 nm. The high reflectance region of the SAM extends from 1480 to 1575 nm. It should be noted that a

considerable lattice-mismatch exists between the ternary quarter-wave layer (lattice constant,  $d=0.587$  nm) and the remaining GaAs/AlAs layers ( $d=0.565$  nm). X-ray diffraction measurements suggest that the strain at the ternary/binary interface is being partially accommodated by dislocations some of which are deep within the mirror structure as indicated by splitting of the diffracted orders resulting from the periodicity of the distributed Bragg reflector. Various attempts to characterize the linear optical properties of the intra-mirror quantum wells were made using room- and low-temperature photoluminescence spectroscopy and photo- and piezo-reflectance spectroscopy. Unfortunately, we were unable to obtain any quantitative information concerning the spectral position and shape of the actual quantum well bandedge. The lack of a well defined bandedge and excitonic features indicates there is some degradation of the quality of the quantum well region of the ternary quarter-wave layer resulting in poor linear optical properties. However, the poor lattice structure may result in a faster recovery of the SAM nonlinear response and improve its performance at the high intracavity intensity levels and repetition rates typical of femtosecond solid-state laser systems.

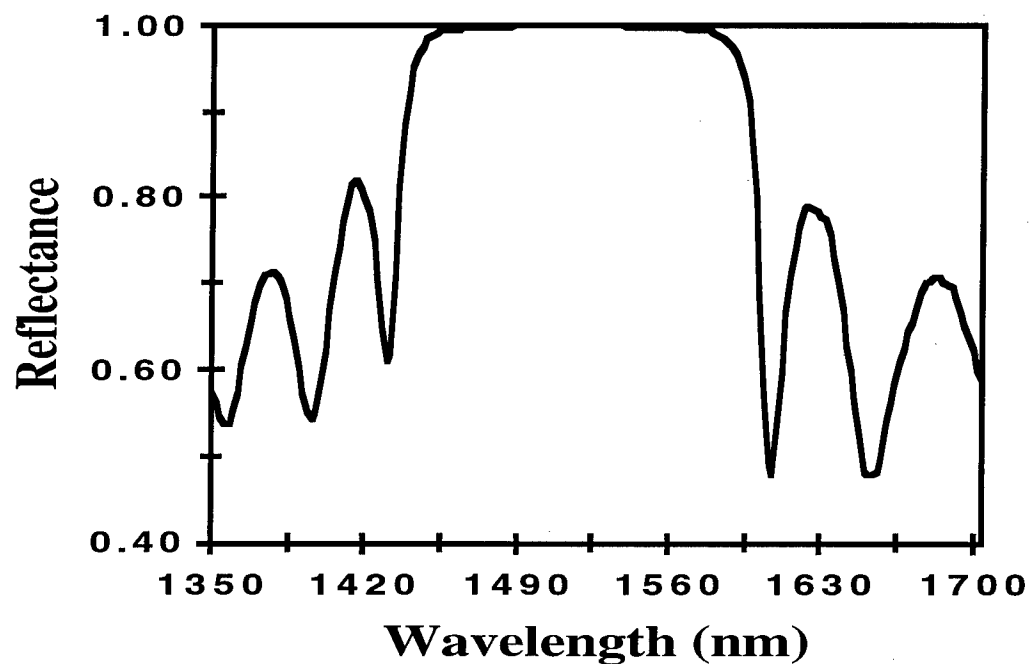


Figure 5. Reflectance spectrum of the saturable absorber mirror

The mode-locked cavity is shown in Figure 6 and is similar to the cw cavity discussed previously. The SAM was placed at the focus of a 10 cm ROC high reflector in the high reflector arm of the cavity. Two fused silica Brewster-cut prisms set at minimum deviation (295 mm tip-to-tip separation) were used in the output arm of the cavity to compensate excess positive group-velocity dispersion introduced by the crystal and mirror coatings. A plane-wedged 1% output coupler was used in this configuration. The overall cavity length remained approximately 1.58 m corresponding to a repetition rate of 95 MHz. Mode-matching between the Nd:YAG pump beam and the laser beam was achieved using a 17.5 cm focal length, AR coated lens.

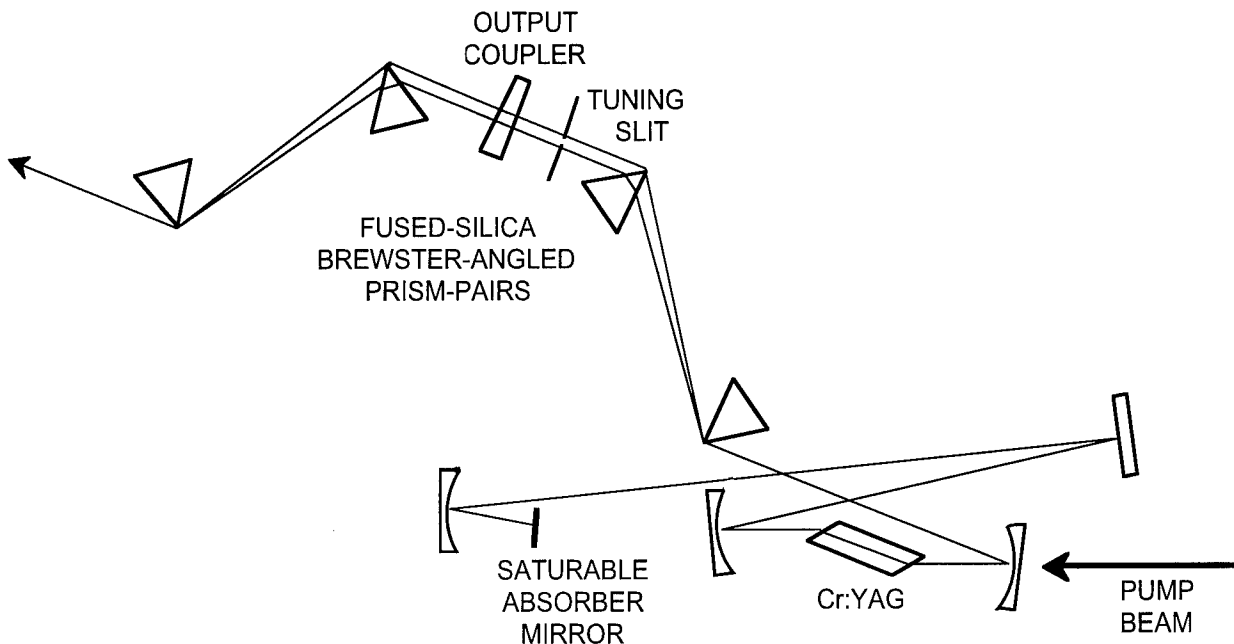


Figure 6. Schematic of mode-locked  $\text{Cr}^{4+}$ :YAG laser X-cavity

Self-starting mode-locking was readily achieved upon alignment of the laser cavity containing the SAM. The pulse width, optical spectrum and pulse train were simultaneously monitored to ensure the presence of stable mode-locking. An Inrad 5-14B, non-collinear autocorrelator was used to determine the pulse width, and a calibrated spectrometer/InGaAs diode array was used in conjunction with an optical multichannel analyzer to monitor the mode-locked

spectrum. The mode-locked pulse train was monitored using a high speed InGaAs detector. Without the dispersion compensating prisms and tuning plate in the cavity, pulse widths on the order of 1 ps centered at 1514 nm were observed. The tuning plate could not be used in conjunction with the SAM because it appears to limit the spectral bandwidth of the Cr<sup>4+</sup>:YAG laser resulting in very unstable operation. The insertion of the fused silica prisms provided the necessary dispersion compensation and femtosecond pulses were readily generated. The absorbed pump power threshold for lasing and self-starting modelocking was 2.7 W. The position of the SAM relative to the 10 cm ROC focusing mirror was optimized to produce a stable, single pulse per cavity round trip pulse train. Optimum stability was achieved when the average output power was between 40 and 80 mW corresponding to an absorbed pump power of approximately 3.0 W. It should be noted that mode-locking was stable over long periods of time and even remained mode-locked during fluctuations in the Nd:YAG pump power. Pulse train instability and multi-pulsing were present when the average output power of the Cr<sup>4+</sup>:YAG laser exceeded 90 mW. Figure 7 shows a typical intensity autocorrelation and mode-locked spectrum at a center wavelength of 1498 nm and an average output power of 45 mW. Assuming a sech<sup>2</sup> intensity profile, the FWHM pulse width was determined to be 122 fs. The corresponding FWHM spectral width was determined to be 20 nm. The time-bandwidth product is 0.33, indicating that the pulses are nearly bandwidth limited.

By inserting a vertical slit into the cavity between the second prism and the output coupler we were able to widely tune the laser while maintaining femtosecond mode-locked operation. The laser was tunable between 1488 and 1535 nm. Figure 8 shows the FWHM pulse width and spectral width of the Cr<sup>4+</sup>:YAG laser as a function of center wavelength. The wide tunability of the laser was readily achieved by careful optimization of the cavity (including pump lens position, folding mirror separation and separation between the focusing mirror and SAM) as it was tuned away from the free-running wavelength of 1510 nm. The Nd:YAG pump power was also increased as required so that the optimal average output power of 40 to 80 mW was maintained. The time-bandwidth product varied from a high of 0.33 to a low of 0.28 indicating nearly

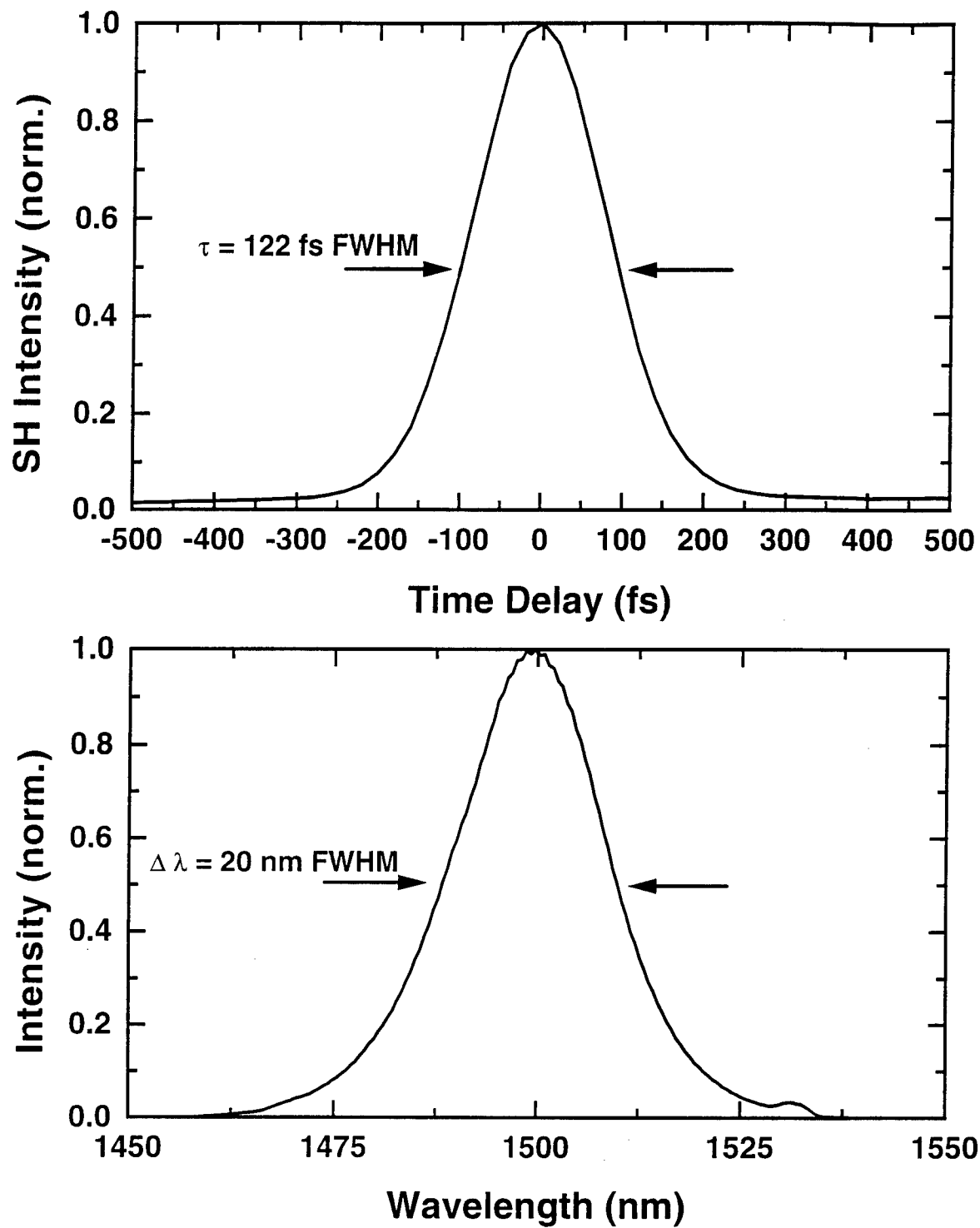


Figure 7. Intensity autocorrelation and mode-locked spectrum of femtosecond pulse at a center wavelength of 1498 nm with an average output power of 45 mW



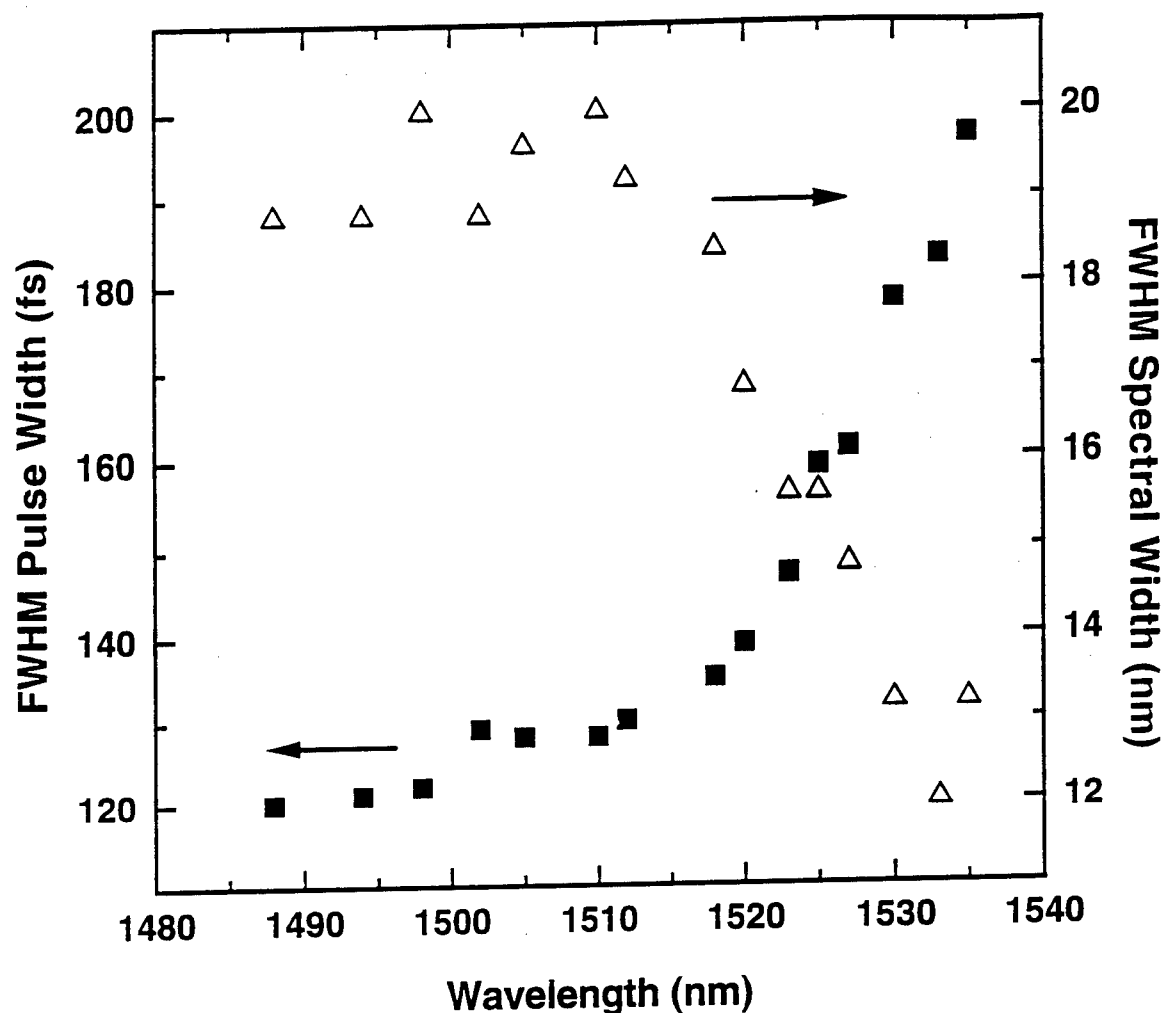


Figure 8. Femtosecond tuning curve of  $\text{Cr}^{4+}$ :YAG mode-locked laser

transform limited pulses over the entire tuning range. It should be noted that stable mode-locking was achieved over the entire tuning range except at the very extreme wavelengths of both the short and long wavelength regions. At these wavelengths, mode-locking was achieved for only brief time intervals. The tuning range on the short-wavelength side is limited by the widely scattered vibrational and rotational  $\text{H}_2\text{O}$  absorption lines that are present from 1200 to 1700 nm.[11] These absorption lines limit the available spectral bandwidth that is required to support femtosecond pulses. There is a sharp increase in pulse width as the  $\text{Cr}^{4+}$ :YAG laser is tuned past 1515 nm. The

calculated round-trip group delay dispersion (GDD) of the laser cavity ranged from  $-1,700 \text{ fs}^2$  at  $1470 \text{ nm}$  to  $-2,700 \text{ fs}^2$  at  $1550 \text{ nm}$ . [12,13] The round-trip third order dispersion (TOD) was also calculated and estimated to be approximately  $+13,500 \text{ fs}^3$  throughout the tuning range of the laser. However, as shown by Brabec *et al.*, the pulse widths are such that the presence of TOD does not limit the formation of femtosecond pulses at these longer wavelengths. [14] Therefore another mechanism is responsible for the increase in pulse width. The efficiency of the saturable absorber ‘falls off’ at longer wavelengths as we tune past the heavy-hole excitonic absorption resonance of the quantum wells which is located at approximately  $1500 \text{ nm}$ . Theimer *et al.*, have recently shown that a decrease in the efficiency of the saturable absorber will limit femtosecond pulse formation at these longer wavelengths. [15]

In conclusion, we have demonstrated both continuous wave and mode-locked operation of a solid-state  $\text{Cr}^{4+}$ :YAG laser. The cw laser was tunable from  $1450$  to  $1574 \text{ nm}$  with output powers exceeding  $600 \text{ mW}$ . The use of a saturable absorber mirror structure provides a very novel and efficient way to effectively mode-lock the  $\text{Cr}^{4+}$ :YAG laser. Tunable femtosecond pulses were generated from  $1488$  to  $1535 \text{ nm}$ . Average  $\text{TEM}_{00}$  output powers ranged from  $40$  to  $80 \text{ mW}$ . A minimum pulse width of  $120 \text{ fs}$  was measured at  $1488 \text{ nm}$ . The femtosecond pulse train is highly stable and is not critically dependent upon cavity alignment. The use of the SAM should prove to be an attractive alternative to KLM techniques in terms of its ease of alignment and long term stability.

### **3. Investigation of Synchronized Mode-Locked Fiber Lasers**

With optical data streams achieving rates in excess of a terabit, all-optical synchronization of fiber lasers for optical clock recovery has become an area of increasing interest. [16,17] This method of synchronization utilizes an incoming optical signal or pulse train to drive a mode-locked laser, which in turn generates a pulse stream at the same rate as the incident signal. This signal can then be used for further optical processing of the data stream. Passively mode-locked lasers conveniently provide short pulses, but they suffer from low repetition rates and relatively large

timing jitters. A possible solution would be to seed a series of passive lasers by an incoming signal so the individual lasers can run at their lower frequencies but combined would provide the data rates required. In addition to locking the laser to the master signal, timing jitters in passively mode-locked lasers has been shown to be reduced in some instances by injection locking.[18,19] Therefore, a set of  $N$  synchronized lasers could provide the base for a distributed time division system with a common clock at the higher optical rates.

The experimental system required a passively mode-locked laser to be slaved to a series of injection pulses acting as the master signal. The source of the pulses or master laser was an actively mode-locked fiber ring laser shown in Figure 9a. The output was in a definite polarization state defined by the polarization controller and the modulator. The Mach-Zehnder modulator also mode-locked the ring laser at harmonics of the fundamental cavity frequency. The cavity length was adjusted until the fundamental frequency of the master laser agreed with the slave laser's frequency of 3.5435 MHz within 100 Hz. By adjusting the polarization paddles within the cavity, pulsewidths of 2 ps were obtained. These pulses acted as the injection signal to the passively mode-locked laser. With the addition of the erbium-doped fiber amplifier, the injection signal reached input powers up to 10 mW.

Most fiber laser synchronization schemes utilize a fiber ring laser configuration for the passively mode-locked system.[18,20] However, the synchronization of a linear fiber cavity was recently reported by Min Jiang *et al.*[21] We employed a standing wave erbium fiber laser in a Fabry-Perot configuration as illustrated in Fig. 9b. The input and output was taken through a fiber Bragg grating which also served as a mirror for the cavity. The grating had a reflection of 50% at the operating wavelength of 1555 nm. A multiple quantum well (MQW) saturable absorber acted as the mode-locking element and as the second mirror for the laser. We eliminated the need for bulk optical mounts by epoxying the MQW saturable absorber to a cleaved fiber end, which allowed us to operate in an all-fiber system.

The master signal was introduced through the fiber Bragg grating via a 50/50 coupler. The output was taken through the unused port and sent to the diagnostic equipment. The MQW laser

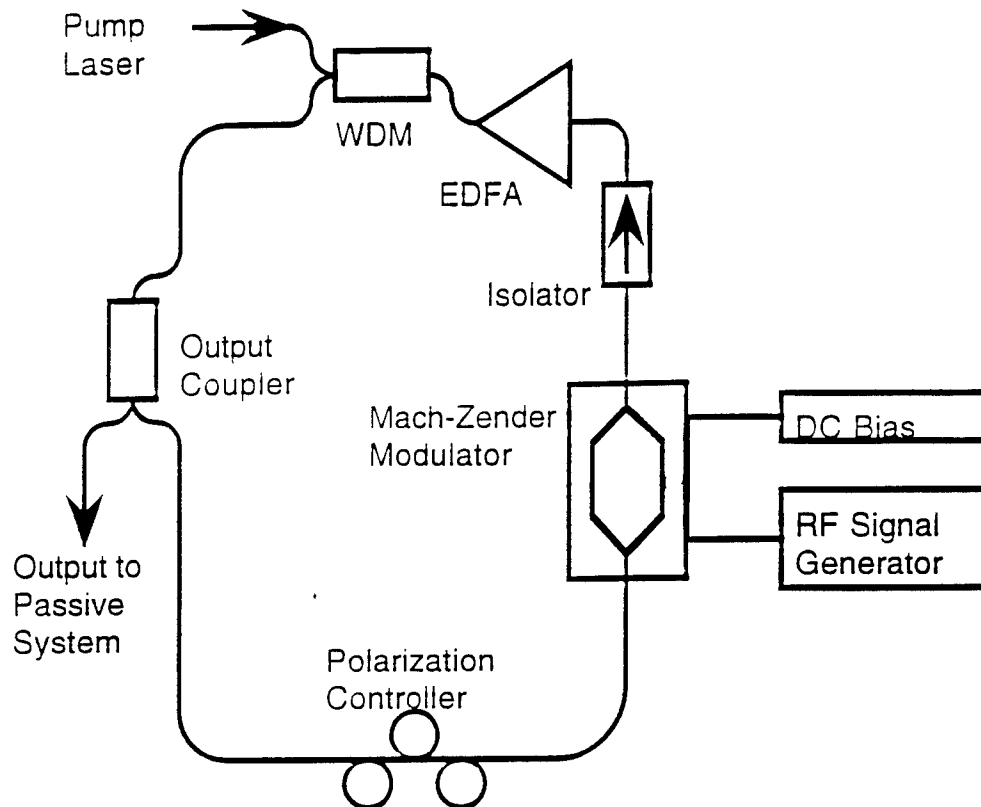


Figure 9a. Schematic of the fiber ring laser used as the 'master' laser. The output from this laser was used to synchronize the passive laser.

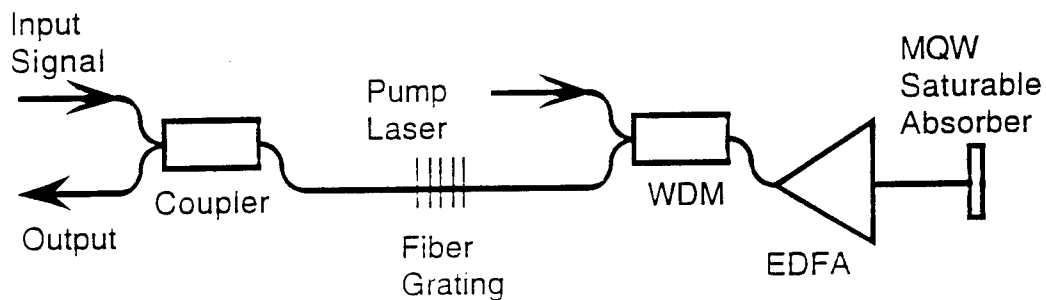


Figure 9b. Layout of the linear cavity employing multiple quantum well saturable absorber and fiber Bragg grating. The injected signal as well as the synchronized output are taken out through the fiber grating.

produced output in a completely random polarization state as none of the elements are polarization sensitive. Spectral and temporal results were observed and multiple stable operational regimes were recorded.

Mode-locked synchronized operation was maintained at the fundamental frequency with average injection powers as low as 1.3 mW, which corresponds to pulse energies of 360 pJ. Below this level the master laser signal was insufficient to initiate synchronized behavior in the slave laser. No discernible difference in operation was observed in the synchronized output when the injected power was increased above this threshold. The synchronized output is shown in Figure 10. The smaller pulses are from the ring laser with the larger being the slaved output from the MQW laser.

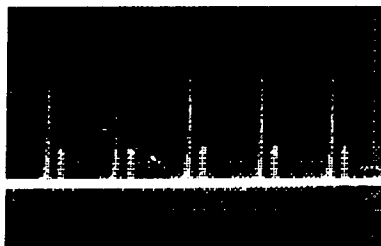


Figure 10. Synchronized output as seen on a digitizing oscilloscope. The pulses are at an identical rate of 3.5435 MHz. The smaller pulses are from the ring laser and the larger pulses are the synchronized output of the slave laser.

Stable operation was determined in part by the position of the incident light on the surface of the saturable absorber. By adjusting the fiber's location and distance from the surface of the MQW saturable absorber, differing regimes could be observed. Operating unsynchronized in a mode-locked state, the passive MQW laser produced 7 ps pulses with a spectral width of 0.45 nm. This gives a time-bandwidth product of 0.4, which is somewhat greater than the 0.31 value corresponding to hyperbolic secant pulses. The synchronized output produced three distinct stable

pulse outputs with pulse widths of 10, 15, and 30 ps shown in Figure 11. The optical spectrum remained stable in all three regimes with a bandwidth of 0.32 nm at FWHM.

Stable operation of a novel synchronization scheme has been achieved. As an application to current communication needs, pulse timing and amplitude stability are critical parameters in assessing potential system performance. This is true for time multiplexed versions in particular. RF noise analysis can provide an initial estimate of the jitter and amplitude fluctuations of all three laser systems: passive, active, and hybrid.

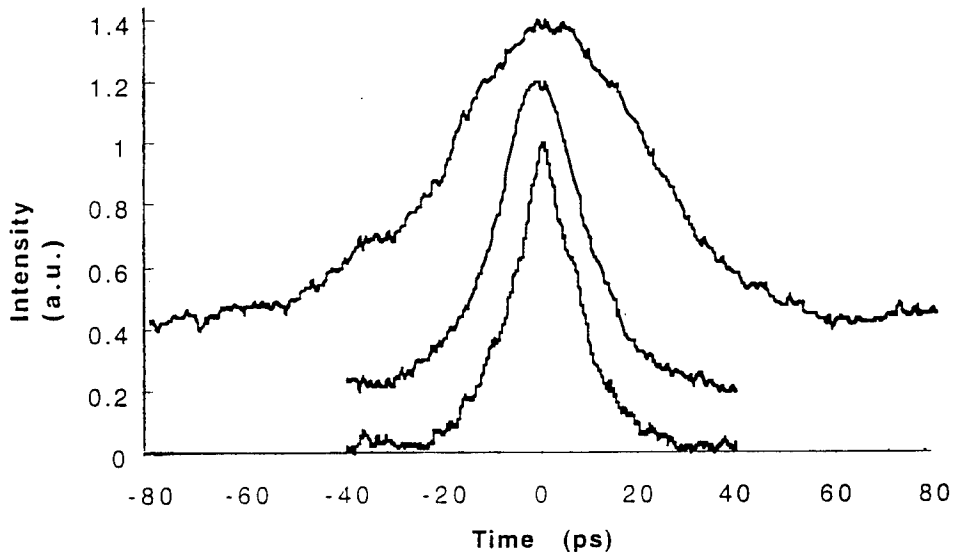


Figure 11. Autocorrelation traces of the synchronized output in three stable operating regimes. The pulses have a common spectral bandwidth of 0.32 nm.

#### **4. Linear Optical Properties of Quantum Well Structures Near 1550 nanometers**

Erbium-doped fiber lasers have become an important laser technology due to their inherent

compatibility with fiber-based optical interconnects, as well as their compact and robust packaging options. In particular, mode-locked fiber ring laser sources producing transform limited optical pulses as short as 77 fs have been demonstrated.[22,23] The ring lasers rely on the use of nonlinear polarization rotation as the mode-locking mechanism and require careful optimization of the round-trip dispersion to produce reliable performance.[24] Standing-wave fiber lasers which utilize a semiconductor multiple quantum well (MQW) saturable absorber as one reflector are an alternative to the ring cavity design.[25] The MQW mirror acts as a saturable absorber mirror due to the intensity dependence of the reflection coefficient. The linear optical properties of the MQW saturable absorbers appear to limit the mode-locking characteristics of the fiber lasers. A thorough analysis of the optical properties including linear absorption and photoluminescence of different MQW samples is presented. This analysis will lead to improved design and growth of future MQW saturable absorbers resulting in reliable and stable picosecond pulse formation in the standing-wave fiber lasers.

The linear optical properties of three MQW saturable absorbers were analyzed. Figure 12 shows the experimental setup used to characterize the linear absorption spectra. A tungsten bulb was used as the white-light illumination source. The intensity of the light was controlled with a variable iris and a RG 850 filter was used to pass only the near IR portion of the tungsten output. The incident light was focused onto the sample with a 50 mm focal length lens. The transmitted light was collected and collimated also with a 50 mm focal length lens. Reflected light off of the surface of the sample passed back through a non-polarizing beam splitter onto a card placed a small distance away from the beam splitter. The focal position of the sample was then adjusted until the best image was observed on the card. A 38 cm focal length lens was then used to focus the collimated light into the ARC 0.275 meter triple grating spectrometer. A germanium detector collected the dispersed light. The detector was then connected to a transimpedance amplifier followed by a SRS 510 lock-in amplifier. A computer program controlled the spectrometer and collected the lock-in transmission data.

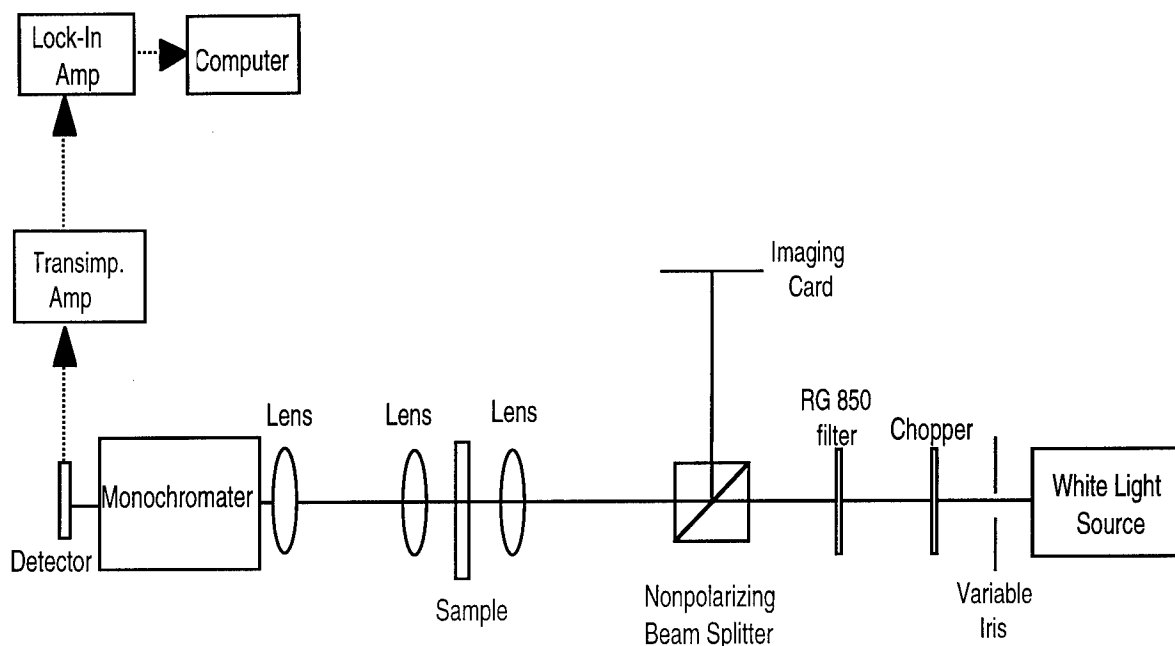


Figure 12. White-light linear absorption experimental setup

The transmission measurements were performed using the following calibration procedure. First a baseline or source measurement was performed with no MQW sample present. Next the transmission through the sample was recorded. The absorbance,  $\alpha L$  of the quantum wells is found from Beer's law and is given by

$$\alpha L = -\ln (I / I_0) \quad (1)$$

where  $I$  is the transmission through the MQW sample and  $I_0$  is the source transmission. The absorption coefficient is found by simply dividing the absorbance by the total thickness  $L$  of quantum well region. The absorbance spectra of the three saturable absorber samples, absorbance versus wavelength are plotted in Figure 13.



Sample #1590 exhibits very well resolved room-temperature light- and heavy-hole excitonic features at 1560 and 1580 nm, respectively. The light- and heavy-hole excitonic

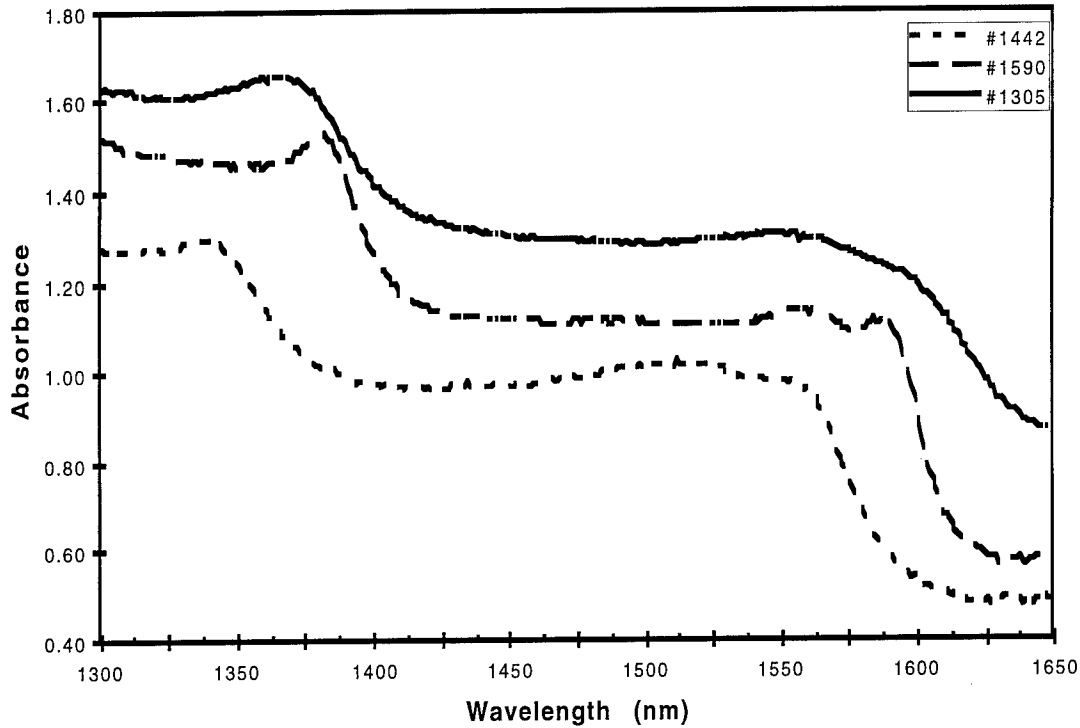


Figure 13. Linear absorbance of MQW saturable absorbers

features of sample #1442 are located at approximately 1520 and 1555 nm, respectively but they are less resolved. Sample #1305 exhibits very indistinguishable excitonic features. The bandedge of #1305 is also located at slightly longer wavelengths than #1442. The unresolved excitonic features of #1305 indicate that many lattice defects are present within the structure. These defects were formed during the MBE growth of #1305. The very broad excitonic features of #1442 indicate that lattice defects are present but to a much lesser extent than in #1305. It should be noted that the absorbance of #1305 is slightly higher than the other two samples especially at the longer wavelengths. This is an experimental artifact due to light leaking around the very small piece of #1305 used to make the transmission measurements. Elimination of the light not being

seen by the sample would be expected to bring the absorbance down to levels comparable with the other samples.

Room temperature photoluminescence experiments were also performed to further analyze the linear optical properties of the saturable absorbers. The photoluminescence experimental setup is shown in Figure 14. The experimental setup is the same as for the linear absorption measurements except that an Ion Laser Technology argon-ion laser producing 100 mW at 515 nm was used as the pump source. The photoluminescence results for samples #1305, #1442, and #1590 are shown in Figure 15.

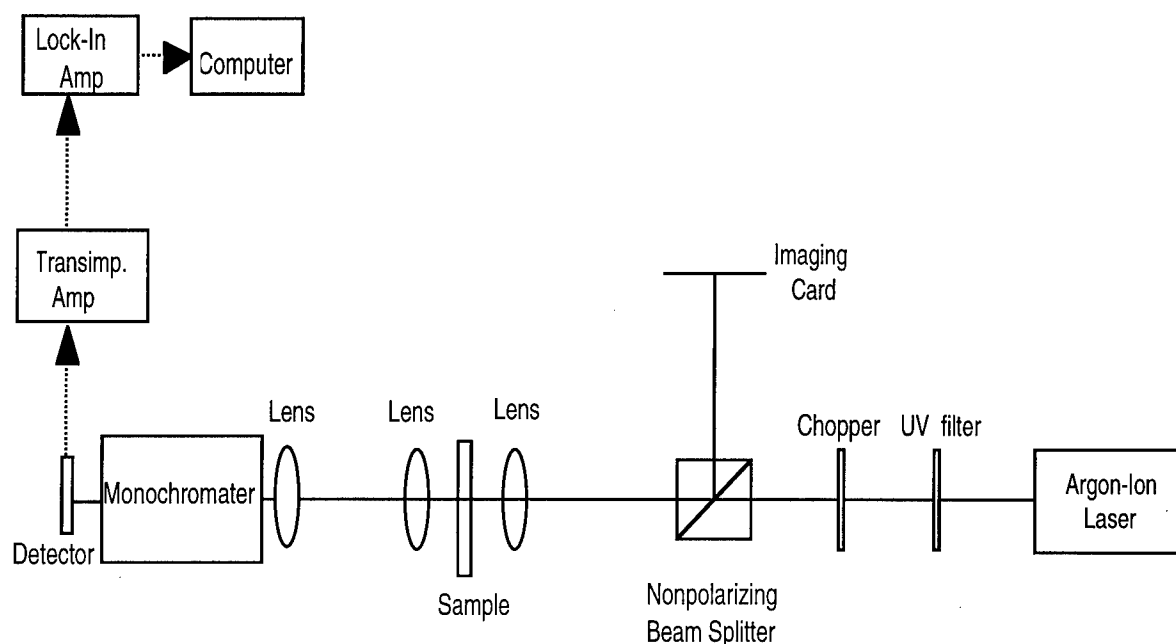


Figure 14. Photoluminescence experimental setup

Sample #1590 has the largest photoluminescence signal and is centered at 1570 nm. The large signal is most likely the result of the well grown material and is directly correlated with the finely resolved excitonic features observed in the absorbance measurements. The next largest signal was obtained from #1442. The photoluminescence peak is centered at approximately 1560 nm. The decreased signal relative to #1590 is due to its more rounded excitonic features. Sample

#1305 displays a very small photoluminescence signal. The peak of this signal is located near 1600 nm. This signal is approximately an order of magnitude less than the signal obtained from #1442.

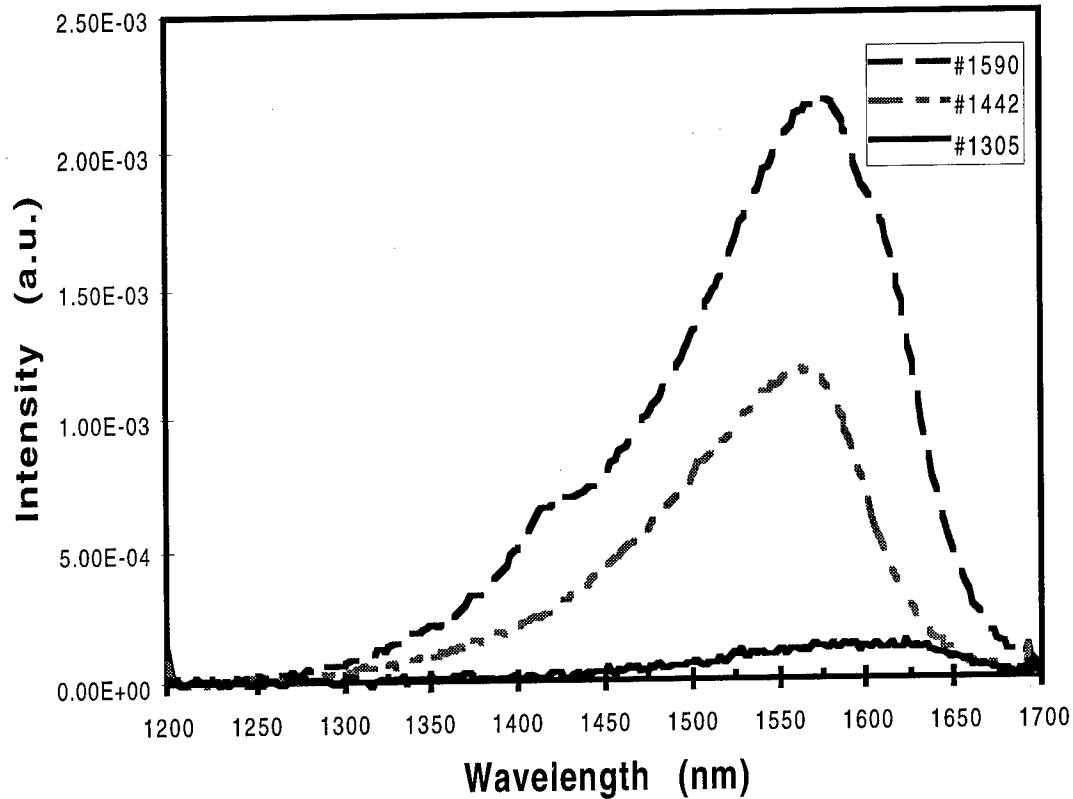


Figure 15. Photoluminescence spectra of MQW saturable absorbers

The mode-locking behavior of the three saturable absorbers was investigated using a standing-wave linear cavity erbium-doped fiber laser.[26] The MQW mirror acts as a saturable high reflector within the laser cavity. Sample #1305 easily mode-locked the fiber laser producing 6 ps pulses with a spectral width of 0.3 nm. The corresponding time-bandwidth product is 0.21 which is close to the transform limited product of 0.22 for a Lorentzian pulse-shape. Sample #1442 and #1590 were also used as the cavity high reflector in an attempt to initiate mode-locking

of the laser. After repeated attempts with both samples, complete mode-locking was not achieved with either sample. Only very broad picosecond pulsing and Q-switching behavior was observed.

Therefore the optical properties exhibited by sample #1305 are ideal for the initiation of passive mode-locking in a fiber laser. The weakly defined excitonic features of #1305 and its low photoluminescence signal indicate that the MQWs contain many lattice defects incorporated during growth. These defects appear to be beneficial to the mode-locking process. Sample #1442 and #1590 seem to contain far fewer defects, but they cannot initiate reliable mode-locking. The lattice defects shorten the carrier lifetime of the electron-hole pairs produced by the absorption of the lasing signal. There is apparently a direct correlation between short-lifetime saturable absorbers and its ability to effectively mode-lock a fiber laser.

The effects of different carrier lifetimes on the initiation of mode-locking needs further investigation. Future planned work involves the use of the femtosecond  $\text{Cr}^{4+}$ :YAG laser to perform pump/probe experiments to quantify the carrier lifetimes of the saturable absorbers. The incorporation of controllable lattice defects into the MQW samples will also be investigated. Sample #1305 contains many defects resulting from poor MBE growth. However this poor growth is uncontrollable and not strictly repeatable. The use of mode-locked fiber lasers in actual optical interconnect systems requires predictable operation of the laser. Unrepeatable growth of the MQW saturable absorbers makes the current laser system impractical. The tailoring of future MQW growth to match the optical parameters of #1305 must therefore be thoroughly investigated. One option is to grow these MQWs at low temperature. This process is repeatable and results in very short carrier lifetimes. Another possible choice is the use of ion implantation as a post-growth process of the MQWs which also results in short carrier lifetimes. The effects of these processes in finding optimal mode-locking parameters should result in the production of reliable mode-locked fiber lasers which could be directly used in optical interconnect architectures.

## 5. References

1. R. K. Boncek, P. R. Prucnal, M. F. Krol, S. T. Johns, and J. L. Stacy, Opt. Eng. **31**, 2442 (1992).
2. M. J. Hayduk, S. T. Johns, M. F. Krol, C. R. Pollock, and R. P. Leavitt, submitted for publication Opt. Commun. Sept. 1996.
3. W. Kaechele, M. F. Krol, and J. W. Haus, submitted to AeroSense '97, Orlando FL., April 1997.
4. M. F. Krol, M. J. Hayduk, S. T. Johns, K. Teegarden, and G. Wicks, SPIE Vol. 2749, 47 (1996).
5. A. V. Shestakov, N. I. Borodin, V. A. Zhitnyuk, A. G. Ohrimtchyuk, and V. P. Gaponstev, in *Conference on Lasers and Electro-Optics*, Vol. 10 of 1991 OSA Technical Digest Series (Optical Society of America, Washington, D. C., 1991), paper CPDP11.
6. P. M. W. French, N. H. Rizvi, J. R. Taylor, and A. V. Shestakov, Opt. Lett. **18**, 39 (1993).
7. Y. P. Tong, J. M. Sutherland, P. M. W. French, J. R. Taylor, A. V. Shestakov, and B. H. T. Chai, Opt. Lett. **21**, 644 (1996).
8. A. Sennaroglu, C. R. Pollock, and H. Nathel, Opt. Lett. **19**, 390 (1993).
9. D. Kopf, G. Zhang, R. Fluck, M. Mosser, and U. Keller, Opt. Lett. **21**, 486 (1996).
10. B. C. Collings, J. B. Stark, S. Tsuda, W. H. Knox, J. E. Cunningham, W. Y. Jan, R. Pathak and K. Bergman, Opt. Lett. **21**, 1171 (1996).
11. D. A. Gilmore, P. Vujkovic Cvijin, and G. H. Atkinson, Opt. Commun. **103**, 370 (1993).
12. R. L. Fork, O. E. Martinez, and J. P. Gordon, Opt. Lett. **9**, 150 (1984).
13. W. L. Bond, J. Appl. Phys. **36**, 1674 (1964).
14. T. Brabec, Ch. Spielmann, and F. Krausz, Opt. Lett. **17**, 748 (1992).
15. J. P. Theimer, J. W. Haus, M. F. Krol and M. J. Hayduk, to be submitted to Opt. Commun..
16. E. Yamada, E. Yoshida, T. Kitoh, and M. Nakazawa, Elec. Lett. **31**, 1342 (1995).

17. P. A. Morton, V. Mizrahi, G. T. Harvey, L. F. Mollenauer, T. Tanbunek, R. A. Logan, H. M. Presby, T. Erdogan, T. Sergeant, and K. W. Wecht, *IEEE Phot. Tech. Lett.* **7**, 111 (1995).
18. M. Margalit, M. Orenstein, and G. Eisenstein, *Opt. Lett.* **20**, 1877 (1995).
19. J. K. Lucek, and K. Smith, *Opt. Lett.* **18**, 1226 (1993).
20. K. Smith, and J. K. Lucek, *Elec. Lett.* **28**, 1814 (1992).
21. Min Jiang, W. Sha, L. Rahman, B. C. Barnett, J. K. Andersen, M. N. Islam, and K. V. Reddy, *Opt. Lett.* **21**, 809 (1996).
22. K. Tamura, E. P. Ippen, H. A. Haus, and L. E. Nelson, *Opt. Lett.* **18**, 1080 (1993).
23. M. Nakazawa, E. Yoshida, T. Sugawa, and Y. Kimura, *Elec. Lett.* **29**, 1327 (1993).
24. K. Tamura, C. R. Doerr, H. A. Haus, and E. P. Ippen, *IEEE Phot. Tech. Lett.* **6**, 697 (1994).
25. R. K. Erdmann, S. T. Johns, and K. J. Teegarden, *SPIE Proceedings*, Vol. 2073, 20-29 (1993).
26. K. J. Teegarden, and R. K. Erdmann, *SPIE Proceedings*, Vol. 2481, (1995).

## 6. Acknowledgments

The authors would like to acknowledge Clifford Pollock and Martin Jaspen of Cornell University for their useful discussions concerning mode-locked solid-state lasers and Rich Leavitt and Rich Tober of the U. S. Army Research Laboratory for the fabrication of the saturable absorber mirror structure.

Also, Kenneth Teegarden of the University of Rochester for his construction of the standing-wave fiber laser used in the synchronization experiments and for the characterization of the saturable absorbers. Joseph Haus of Rensselaer Polytechnic Institute and Reinhard Erdmann of Rome Laboratory for useful discussions concerning the dynamics of fiber lasers.

Finally, Gary Wicks of the University of Rochester for his fabrication of the MQW saturable absorbers.

***MISSION***  
***OF***  
***ROME LABORATORY***

**Mission.** The mission of Rome Laboratory is to advance the science and technologies of command, control, communications and intelligence and to transition them into systems to meet customer needs. To achieve this, Rome Lab:

- a. Conducts vigorous research, development and test programs in all applicable technologies;
- b. Transitions technology to current and future systems to improve operational capability, readiness, and supportability;
- c. Provides a full range of technical support to Air Force Materiel Command product centers and other Air Force organizations;
- d. Promotes transfer of technology to the private sector;
- e. Maintains leading edge technological expertise in the areas of surveillance, communications, command and control, intelligence, reliability science, electro-magnetic technology, photonics, signal processing, and computational science.

The thrust areas of technical competence include: Surveillance, Communications, Command and Control, Intelligence, Signal Processing, Computer Science and Technology, Electromagnetic Technology, Photonics and Reliability Sciences.